



2

NASA

Technical Memorandum 105794

A Demonstration of an Intelligent Control System for a Reusable Rocket Engine

Jeffrey L. Musgrave and Daniel E. Paxson
Lewis Research Center
Cleveland, Ohio

DTIC
ELECTE
SEP 28 1992

Jonathan S. Litt
Propulsion Directorate
U.S. Army Aviation Systems Command
Lewis Research Center
Cleveland, Ohio

and

Walter C. Merrill
Lewis Research Center
Cleveland, Ohio

U.S. Army Aviation Systems Command
Huntsville, Alabama

Preprint from the "Advanced Earth-to-Orbit Propulsion Technology Conference," a conference held at NASA George C. Marshall Space Flight Center Huntsville, Alabama, May 19-21, 1992

92 9 25 105**NASA**

387544 **92-25954** 11

A DEMONSTRATION OF AN INTELLIGENT CONTROL SYSTEM FOR A REUSABLE ROCKET ENGINE

Jeffrey L. Musgrave
Daniel E. Paxson
NASA Lewis Research Center

Jonathan S. Litt
US Army-AVSCOM

Walter C. Merrill
NASA Lewis Research Center
Cleveland, Ohio 44135

Accession For	
NTIS GRA&I	<input checked="" type="checkbox"/>
DTIC TAB	<input type="checkbox"/>
Unannounced	<input type="checkbox"/>
Justification	
Per Form 50	
Distribution/	
Availability Codes	
Avail and/or	
Dist Statement	
A-1	

ABSTRACT

DTIC QUALITY INSPECTED 3

An Intelligent Control System for reusable rocket engines is under development at NASA Lewis Research Center. The primary objective is to extend the useful life of a reusable rocket propulsion system while minimizing between flight maintenance and maximizing engine life and performance through improved control and monitoring algorithms and additional sensing and actuation. This paper describes current progress towards proof-of-concept of an Intelligent Control System for the Space Shuttle Main Engine. A subset of identifiable and accommodatable engine failure modes is selected for preliminary demonstration. Failure models are developed retaining only first order effects and included in a simplified nonlinear simulation of the rocket engine for analysis under closed loop control. The engine level coordinator acts as an interface between the diagnostic and control systems, and translates thrust and mixture ratio commands dictated by mission requirements, and engine status (health) into engine operational strategies carried out by a multivariable control. Control reconfiguration achieves fault tolerance if the nominal (healthy engine) control cannot. Each of the aforementioned functionalities is discussed in the context of an example to illustrate the operation of the system in the context of a representative failure. A graphical user interface allows the researcher to monitor the Intelligent Control System and engine performance under various failure modes selected for demonstration.

INTRODUCTION

Reusable rocket engines present a very challenging operational environment and requires high performance, low maintenance, and man-rated reliability levels. Multiple start-stop cycles cause thermal gradients with high thermal strains per cycle within the engine. High steady state operating stresses create large inelastic strains. High dynamic loads induce high cycle stresses. In the Space Shuttle Main Engine (SSME), an operational version of a reusable rocket engine, high performance and reliable operation have been achieved. However, originally predicted levels of usable life have not been demonstrated and extensive between flight maintenance has resulted.

Merrill and Lorenzo have proposed a framework outlining specific functionalities to improve the durability of the SSME which include active control of key engine parameters, real time diagnostics, and life extending control².

A functional framework showing the various capabilities included in the Intelligent Control System (ICS) is given in Figure 1. The principal components include a distributed diagnostic system, an intelligent coordinator, and a reconfigurable controller. The distributed diagnostic system is composed of sensor validation, a model based failure detector, a rule based failure detector, ReREDS (reusable rocket engine diagnostic system) and a diagnostic expert system. ReREDS is a condition monitoring/diagnostic software system developed during the past two years through a contract with System Control Technology (SCT) and Aerojet. The engine level coordinator in Figure 1 makes alterations to the controller using engine status information generated by the diagnostic system, and propulsion requirements passed down by the propulsion level coordinator as shown. Each SSME is part of the propulsion system for the orbiter vehicle and is orchestrated by the propulsion level coordinator which receives thrust vector commands from the flight controller to achieve mission success. Ultimately, the engine level coordinator must satisfy minimum thrust requirements while minimizing further component degradation and accommodating failed or degraded engine hardware. The reconfigurable controller takes requests generated by the coordinator, makes the changes gradually thereby minimizing engine transients, and computes the valve positions to achieve the requested behavior from the engine.

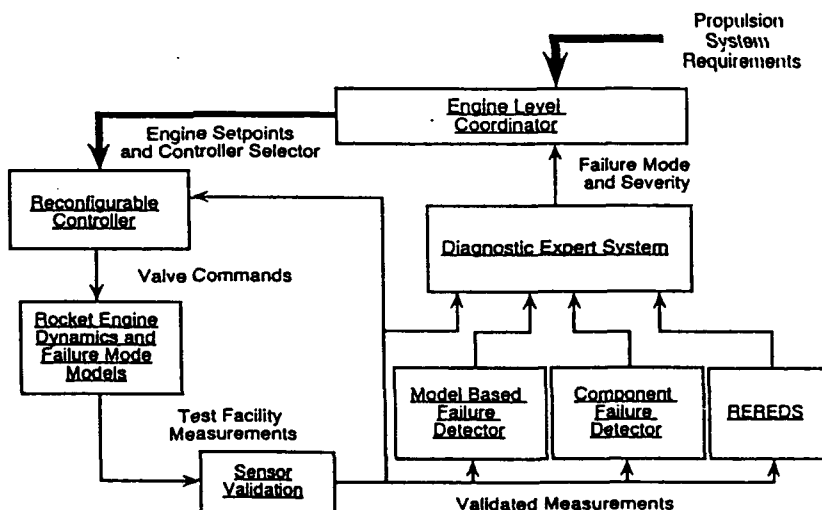


Figure 1 Intelligent Control System Functional Framework

This paper describes an ongoing research program at the NASA Lewis Research Center to demonstrate an ICS for a reusable space propulsion system (SSME). A significant milestone for the ICS program is the successful integration of real time diagnostics with a reconfigurable control³ providing motivation for demonstration with a subset of accommodatable failure modes. The focus of this work is on failure mode modelling, controls and coordination, and the graphical user interface. Detailed discussion of the distributed diagnostic system appears elsewhere⁴. An accommodation strategy for a particular failure mode is discussed in detail and simulation results are presented to clarify the various functionalities and potential benefits of the Intelligent Control System.

FAILURE MODES

Modelling failure modes for the ICS project presents a difficult challenge due to several competing objectives. On the one hand there is the desire to accurately describe the progress and effects of a given failure as it occurs. Typically, this requires models not only for the relevant fluid dynamics but for the structural dynamics as well. Such models are necessarily computationally intensive and time consuming to develop. On the other hand, there is the desire to maintain simple models such that real time simulation may be achieved with existing computer hardware. The real time requirement is necessitated by the fact that the diagnostic system and controller under development will eventually be placed on an actual engine, and must therefore respond within the appropriate time scale. Simple failure models also require much less time to develop and are readily available for use in detection and accommodation studies for development of an expert system rule base.

At this point in time, the focus of the project is proof of concept. Therefore, a philosophy of maximum simplicity has been adopted for the task of modelling rocket engine failures. By this we mean that the consequences of a given failure are sought without regard to the cause or the relative time that the failure takes to develop. The following discussion details models for several failure modes selected for demonstration of an ICS. Motivation for their selection will be presented, along with a description of their implementation in the real time simulation model of the SSME⁵. In addition, open loop transients of key engine parameters are provided to illustrate the qualitative behavior of the models.

FAILURE MODE SELECTION

The following five failure modes have been selected for the preliminary ICS demonstration: a failure of a control sensor (P_c), a frozen Fuel Preburner Oxidizer Valve (FPOV), a Low Pressure Fuel Turbo Pump (LPFTP) shaft seal system failure, a High Pressure Fuel Turbo Pump (HPFTP) turbine tip seal failure, and a High Pressure Oxidizer Turbo Pump (HPOTP) shaft seal system failure. One of the primary goals of the project is to examine a variety of techniques for failure detection and accommodation since no one is expected to perform well for all types of failures. The modes listed above cover a broad class of possible problems for the engine with the exception of bearing failures. Unfortunately, the real time engine simulation used for this work does not readily lend itself to including failure modes involving vibration, or other structural phenomena.

Sensor failures and actuator failures are among the most straight forward to implement and require no modelling. Consequently, they have been omitted from the following discussion. The HPOTP shaft seal failure has been covered extensively elsewhere⁶ and will not be repeated here.

FAILURE MODE MODELLING

LPFTP Shaft Seal System Failure. The LPFTP shaft seal system prevents the relatively hot hydrogen gas which drives the low pressure turbine from mixing with the liquid hydrogen being driven through the low pressure pump. The seal system consists of two seals. One is a labyrinth seal located at the base of the second stage turbine blade. The other is a simple ring seal on the shaft itself. Since both of these are clearance type seals, a small amount of leakage occurs even during normal operation. This value is approximately .49 lbm/sec. Using the perfect gas assumption the flow through the labyrinth seal may be written as

$$\dot{m}_{lab} = \pi C_D d c_{lab} P_{lpti} \sqrt{\frac{g_c}{RT_{lpti}}} f(PR) \quad (1)$$

where C_D is the discharge coefficient, d is the turbine disk diameter, c_{lab} is the seal clearance, g_c is the gravitational constant, R is the real gas constant, T and P are the LPFTP turbine inlet temperature and pressure respectively, and PR is the pressure ratio across the seal, i.e. P_{exit}/P_{lpti} . In this equation $f(PR)$ has the form

$$f(PR) = \sqrt{\frac{1 - PR^2}{5 - \ln(PR)}} \quad (2)$$

Assuming adiabatic flow and choked conditions, the flow through the ring seal may be written as

$$\dot{m}_{ring} = 0.685 \pi C_D d c_{ring} P_{exit} \sqrt{\frac{g_c}{RT_{lpti}}} \quad (3)$$

where d , and c_{ring} now correspond to the shaft diameter and the ring seal clearance respectively. The multiplicative constant .685 is obtained using a specific heat ratio for hydrogen gas of 1.4. Assuming a common discharge coefficient of 0.9 for both seals and disk and shaft diameters of 6.0 and 2.0 inches respectively, equations 1 and 3 may be equated and the common terms eliminated to obtain

$$\frac{C_{ring}}{C_{lab}} = 4.381 \frac{f(PR)}{PR} \quad (4)$$

This equality cannot be rearranged to obtain an analytical expression for the pressure ratio PR as a function of clearance due to the nature of $f(PR)$. However, an approximation can be obtained by expanding equation 4 in a Taylor series about $PR=1$. The result is

$$PR = 2.0 \frac{1 + \sqrt{1 + .75 \beta(PR)}}{\beta(PR)} \quad (5)$$

where $CR = C_{ring}/C_{lab}$ and $\beta(CR)$ is

$$\beta(CR) = 1.303 CR^2 + 7.0. \quad (6)$$

Thus with the clearance of each seal known, and the LPFTP turbine inlet state known, equation 5 may be used to obtain PR. With PR known, P_{exit} is known, and equation 3 may be used to obtain the flow rate through the seal.

The clearance of the ring seal must be specified and a failure of the system is initiated by using a clearance which is much larger (approximately a factor of ten for the demonstration) than the nominal value which is assumed to be 3 mils. The clearance of the labyrinth seal depends upon the speed of the turbine. Specifically, the governing equation may be written as

$$C_{lab} = 0.005 - a_1 (\omega^2 - a_2) \quad (7)$$

where ω is the turbine shaft speed in rad/sec. The constants a_1 and a_2 were chosen such that the clearance is 5 mils at 100 percent power and 0 mils at full power.

The LPFTP shaft seal model has been implemented on the real time SSME simulation by introducing these equations into the code. The mass flow rate through the seal system was subtracted from the low pressure fuel turbine discharge mass flow and added to the pump discharge mass flow. The pump discharge temperature was modified to account for the hot gas mixing with the cold liquid. Figures 2a, 2b, and 2c show the open loop response of the shaft seal failure at rated power. Chamber pressure was insensitive to the shaft seal failure, and has been omitted. The seal degradation is shown on all plots to occur at four seconds and take place over a two second interval at a constant ramp rate. For the failure shown, the leakage rate from the turbine to the pump increased from a nominal 0.486 lbm/sec to 1.66 lbm/sec causing a decrease in the LPFTP pump discharge pressure shown in Figure 2a as the turbine pumps less fuel from the tank. Figure 2b shows how the increase in hot gas entering the cool fuel from the supply tank results in a slight increase in pump discharge temperature. Both the discharge pressure and temperature along with the volumetric fuel flow from the pump and chamber pressure are used to estimate the mixture ratio in the main combustion chamber. Figure 2c shows how the relatively minor leakage causes the mixture ratio estimate to degrade. The degradation is caused by the relatively large drop in the pump discharge pressure. The poor mixture ratio causes some difficulties for the multivariable control approach and is discussed in some detail later. The LPFTP shaft seal failure model provides the qualitative behavior of interest for closed loop analysis and development of accommodation strategies.

LPFTP Turbine Tip Seal Failure. Turbine tip seals are designed to prevent leakage of gas between the outside ends of the turbine blades and

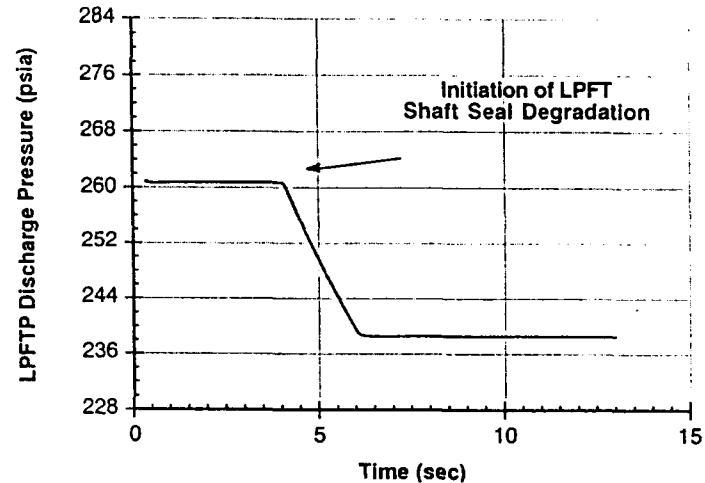


Figure 2a Open Loop Response of LPFTP Discharge Pressure to LPFTP Shaft Seal Degradation

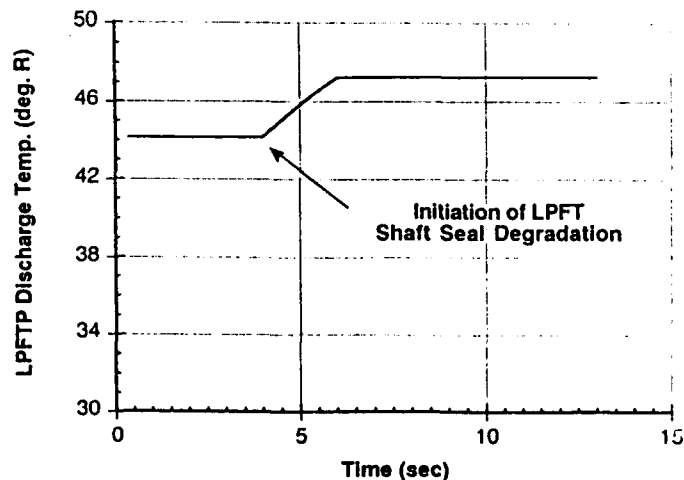


Figure 2b Open Loop Response of LPFTP Discharge Temperature to LPFTP Shaft Seal Degradation

the turbine casing. The rate of leakage which occurs in this region is generally very small compared to the total flow through the turbine; however, the effect on performance can be significant. The fluid leaking around the tip of the turbine blade disturbs the flow field on the rest of the aerofoil in a manner similar to crossflow over an airplane wing. This results in reduced lifting capacity of the blade and therefore reduced efficiency of the turbine. In order to prevent this effect, turbine blades are often shrouded on the ends. The shroud reduces the crossflow and subsequent sensitivity to tip leakage. Furthermore, the shroud is typically equipped with a labyrinth type tip seal which cuts down significantly on the leakage flow. The HPFTP does not have shrouded blades however, due to high speed and inlet temperature. Sealing is therefore affected by maintaining as small a clearance as possible between the blade tip and the housing. A seal failure represents a change in this clearance to some value significantly larger than the design value. Experiments demonstrate⁷ that the relationship between turbine efficiency and tip clearance is generally linear; however, the slope is strongly dependent on the number and degree of reaction of the turbine stages. Although it has been determined to be a relatively likely failure⁸, no actual mention of the cause of the tip seal clearance change has been made or the degree of clearance change that is expected. Figures 3a, 3b, and 3c demonstrate the qualitative behavior of this failure in an open loop simulation of the real time SSME model for a 10% ramp decrease in turbine efficiency beginning at four seconds. Figure 3a shows a relatively slight decrease in chamber pressure resulting from the decrease in the HPFTP pump discharge pressure. The pump discharge pressure drops because the turbine is doing less work on the fluid for the given preburner temperature. Figure 3b shows both the estimated and actual MRs rising because of the drop in fuel being pumped by the HPFTP. Notice the slight degradation in the MR estimate as the failure propagates to its full value at six seconds. This degradation in the estimation scheme does not cause difficulties with the MVC as in the case discussed above. Figure 3c shows a dramatic rise in the HPFTP discharge temperature resulting from the decrease in the turbines ability to remove energy from the hot gas of the preburner. The open loop responses shown in these figures typify behavior for a decrease in efficiency of the high pressure fuel turbine and coincide with our physical understanding of the failure and its impact on performance parameters.

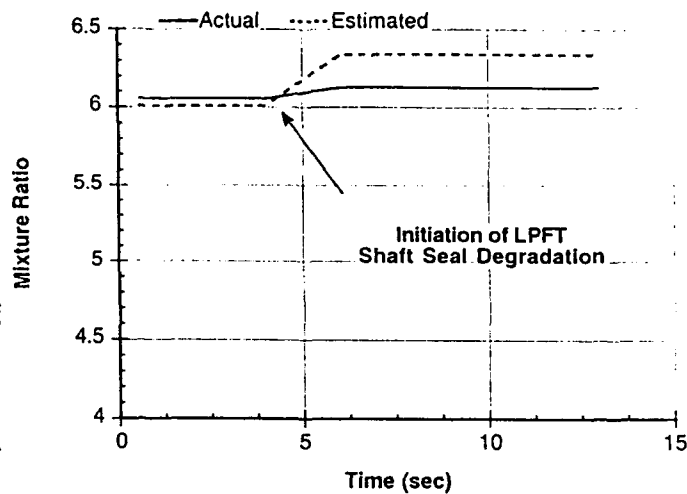


Figure 2c Open Loop Response of Mixture Ratio to LPFT Shaft Seal Degradation

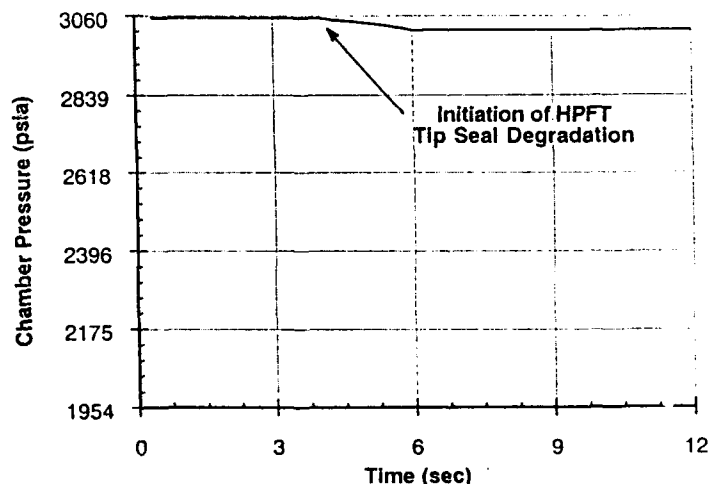


Figure 3a Open Loop Response of Chamber Pressure to HPFT Tip Seal Degradation

CONTROLS AND COORDINATION

The control and coordination functions lie at the heart of the intelligent control system. Selection of failure modes for an on-line diagnostic system is driven by the ability to accommodate such failures or degradations in hardware using existing sensing and actuation. Additional sensing and actuation hardware may be considered by weighting expected costs against benefits in conjunction with the likelihood of the failure occurring and the effect if left unattended. For this work, an additional actuator was selected for inclusion in an engine model based on recommendations from a study performed by Rocketdyne⁹ under contract to NASA LeRC. In addition, the instrumentation set on the Marshall Space Flight Center Technology Test Bed is assumed.

NOMINAL MULTIVARIABLE CONTROLLER

Control of the SSME is accomplished through five valves shown in Figure 4. In particular, the Main Oxidizer Valve (MOV), Main Fuel Valve (MFV), Coolant Control Valve (CCV), Oxidizer Preburner Oxidizer Valve (OPOV), and

Fuel Preburner Oxidizer Valve (FPOV) are open loop scheduled to perform the startup and shutdown operations. In the actual SSME controller (Block 1), only FPOV and OPOV are used as closed loop control valves for mainstage operation. To analytically explore the benefits of enhanced engine controllability, the Oxidizer Preburner Fuel Valve (OPFV) was added while the previous five valves were also considered for closed loop control during mainstage¹⁰.

A number of measurement locations are shown in Figure 4 which represent a subset of the SSME test bed sensor suite. The discharge pressure and temperature of the Low Pressure Fuel Turbopump (P_{t11} and T_{t11} respectively) as well as volumetric fuel flow (Q_{f1m}), and chamber pressure (P_c) are used for estimating mixture ratio (MR) in the existing SSME Block 1 controller. The discharge pressure of the High Pressure Fuel Turbopump (P_{t12}), the discharge temperatures of the High Pressure Fuel and LoX Turbines (T_{t2d} and T_{o2d} respectively), the pressure of the Fixed Nozzle Heat Exchanger (P_4), the pressure of the Main Chamber Heat Exchanger (P_5), and the fuel supply pressure of the preburners (P_9) are used in conjunction with P_c to form the sensor suite for the multivariable control.

Multivariable control (MVC) methods generally rely on linear state space models of the process to be controlled. A perturbation model of a simplified (39 state) nonlinear dynamic engine model at rated power was used for control design¹⁰. The linear models of the SSME change very little from the 65% to the 109% power (thrust) level, therefore gain-scheduling was not required. MVC allows the integration of multiple objectives of P_c , Mr, T_{t2d} , and T_{o2d} command following for example, while decoupling each of the control loops from the others using all six valves in Figure 4 as closed loop control valves.

The nominal controller is designed with the objective of providing the highest degree of fault tolerance and robustness possible for the engine using all available valves and some subset of available sensors while meeting specified performance constraints. Ideally, the sensors selected for state estimation in the state feedback controller would be the most reliable and most accurate of the available instrumentation. However, a performance versus robustness tradeoffs must be made if the most reliable sensors result in a non-minimum phase realization¹⁰.

A fault tolerant and robust control design for a rocket engine may be achieved in two ways using multivariable control. The first involves designing the controller to be insensitive to variations in the engine, modelling errors, and sensor noise. A variety of formalized techniques for accomplishing this are available in the controls literature based upon the design methodology used. The second involves wisely selecting the variables for closed loop control. For example, a "traditional" control design would allow set point control of both P_c and MR to provide variable throttling and near constant combustion temperature in the main chamber over a range of power levels, respectively. However, for a staged combustion cycle, controlling the discharge temperatures of the high pressure turbines provides a means of regulating the combustion temperatures in the fuel and lox preburners. Moreover, discharge temperatures are redline quantities on the SSME. Redline cutoffs resulting from a decrease in fuel turbine efficiency can be avoided¹¹. In general, closed loop control of redline variables may widen the envelope of operation for the engine allowing greater flexibility for off design operation. Consequently, a fault tolerant multivariable control design can be achieved by including T_{t2d} and T_{o2d} in the controlled variable list along with P_c and MR for the set point controller. However, there may be a better choice given typical variations in engine builds and the difficulty of providing consistent and accurate measurements of turbine discharge temperature. The final selection must depend upon the practical aspects of implementing such a design on a flight system.

RECONFIGURABLE CONTROL

The notion of altering the structure of the controller to accommodate changes in the plant is very attractive for

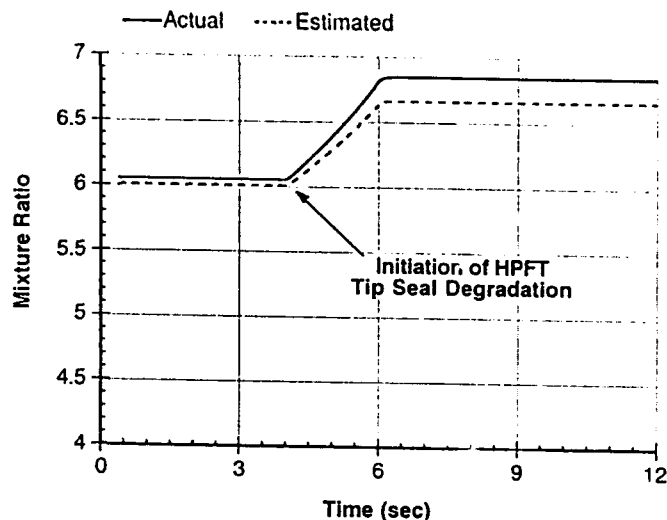


Figure 3b Open Loop Response of Mixture Ratio to HPFT Tip Seal Degradation

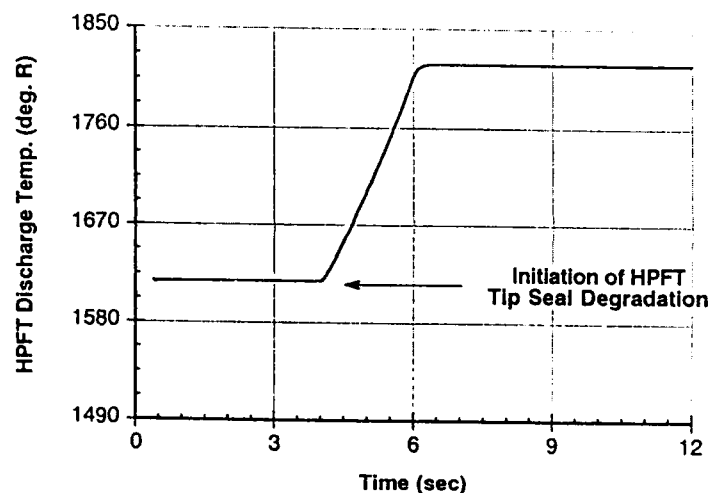


Figure 3c Open Loop Response of HPFT Discharge Temperature to HPFT Tip Seal Degradation

fault tolerance. Much work has been done in the area of aircraft survivability in combat situations with a focus on actuator failures resulting from battle damage¹². However, most approaches are heuristic in nature due to the difficulty in generalizing results from a specific application and vary between apriori and on-line design. A common theme is to distribute the control effort for a failed actuator over the remaining, hopefully somewhat redundant actuators in the system.

The SSME has six valves while the nominal engine controller has only four parameters as controlled quantities. Therefore, it would appear that the engine has two redundant valves for independent control of P_c , MR, T_{ft2d} and T_{ot2d} during mainstage operation since the input matrix of the design model is not rank deficient. However, the nominal control design¹⁰ does not use MOV or MFV for mainstage operation since these two valves are primarily for startup and shutdown. In fact, MOV and MFV are kept wide open for all power ranges encountered during mainstage operation in the Block I controller. Therefore, it was concluded that these valves should not be moved for nominal engine operation by increasing the control weighing in the multivariable design. However, these valves can play a major role in accommodating a failure in one or more of the primary control valves (FPOV, OPOV, CCV and OPFV).

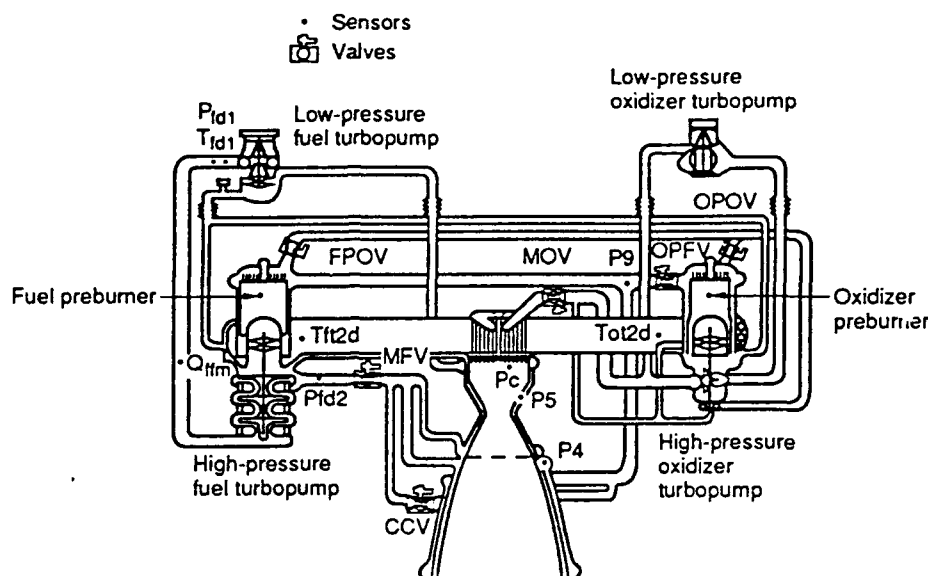


Figure 4 Modified Propellant Flow Schematic of the Space Shuttle Main Engine

One approach for control reconfiguration for actuator failures is shown in Figure 5. The basic idea is to design a controller for each of the failure conditions and then switch designs once the failure is identified by the online diagnostic system. For example, if the position of FPOV sticks at a certain time in the mission, then a control law (u_{fpo}) designed without the column corresponding to FPOV in the B matrix of the design plant is blended with the nominal control (u_{nom}) to give the applied control (u_{app}) as

$$u_{app}(t) = (1-\lambda(t)) u_{nom}(t) + \lambda(t) u_{fpo}(t), \text{ where } \lambda(t) \in [0,1]. \quad (8)$$

As shown in the figure, the nominal and off-nominal control designs run in parallel to minimize startup transients associated with switching between controllers. The approach is straight forward from both a conceptual and implementation standpoint. The difficulty is selecting an acceptable blending rate $\lambda(t)$ between the nominal control and the new control for the failure condition. Once the new controller is active, the closed loop performance and robustness are known from the apriori design. However, the approach has several short comings. The most significant being the high number of parallel controllers of order (N) for a potentially large number of failure scenarios (M) resulting in a control system of order $N \times M$ making implementation of such a system in flight hardware somewhat impractical. Another potential problem involves integrator windup for each of the controllers running in parallel but "off-line". Windup may result in transients of the kind we hoped to avoid by running the controllers in parallel in the first place. However, this behavior has not been a problem to date and can be minimized further by ramping between controllers more slowly. The approach taken is not a panacea, however it does allow us to explore the potential benefits of using control reconfiguration in a relatively straight forward way.

ENGINE LEVEL COORDINATOR

The engine level coordinator may change the setpoints of the currently controlled variables to meet performance constraints, avoid detrimental operating conditions, change the controlled variables (i.e. mode switching), or select an alternate control structure to accommodate a failed or degraded component in the engine system as summarized by Figure 5. Moreover, degradations or failures of certain engine components may adversely affect performance limits. In this situation, the coordinator must recompute new limits based on information provided by the on-line diagnostic system. The engine level coordinator is responsible for meeting thrust and MR requirements set by the propulsion level to the extent possible while avoiding an engine shutdown condition. Engine shutdown is determined by the propulsion level coordination based on information provided by the engine level coordinator, relative health of the remainder of the propulsion system, and mission safety requirements. Information about the health of the engine and the necessary performance parameters are supplied to the propulsion coordinator to aid decision making at that level about each engine's thrust and MR.

A bottom up strategy has been adopted to develop algorithms for use in the engine level coordinator. For the

failure modes considered thus far, only the FPOV sticking has resulted in any identifiable coordination activity. If the valve sticks at some point during the Max Q maneuver, the maximum achievable thrust for the engine will decrease if the MR setpoint is observed. The job of the coordinator is to determine the maximum thrust as a function of the estimated position of the stuck valve and provide this new limit to the controller. The HPFTP turbine tip seal failure could have coordination activity by changing the set points for P_c , $Tft2d$, and $Tot2d$ based on the estimated change in turbine efficiency. However, the MVC reaches a balance without any explicit changes in commands⁹ thereby making the problem one of potential integrator windup. The LPFTP shaft seal failure may require some coordination, but this work must wait until an alternative MR estimation scheme is developed to provide a suitable value for the multivariable control. The HPOTP seal system failures have no direct effect on performance parameters, however off nominal operation such as slowing the pump down may help to avoid further degradations. However, our modelling efforts have not progressed to the level of detail which would allow some reasonable assessment of the effect of speed on seal wear during failure propagation.

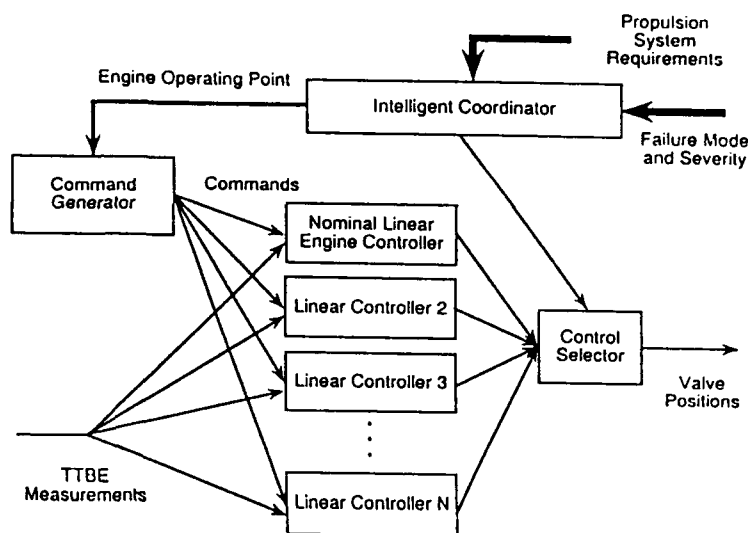


Figure 5 Multivariable Reconfigurable Control Scheme

ACCOMMODATION STRATEGIES

Accommodation strategies have been developed for the sticking of FPOV and the HPFTP turbine tip seal failure. The simulation results for accommodation of the turbine tip seal failure have been published elsewhere¹¹ and will not be repeated here. Further work is required for the LPFTP shaft seal and possibly the HPOTP shaft seal system. The MVC is marginally unstable for a nontrivial leakage in the LPFTP shaft seal when using the MR estimation algorithm developed for the Block I control. The reason for this has roots in the differing design philosophies between Block I and the MVC. The MVC has MR as the "fast" control loop while the Block I control uses P_c as the "fast" loop. Having MR as the faster loop provides better control of temperature deviations in the engine cycle and results in a lower order controller since the MR response is much slower than P_c . Oscillations in the MR response result from the impact of the LPFTP shaft seal failure on the quality of the MR estimate as shown earlier in Figure 3a, while the Block I control experiences no difficulty in regulating P_c and MR. Work is in process to develop an alternative MR scheme using a kalman filter to alleviate the marginal instability with the MVC.

FPOV Sticking. The sticking of the FPOV during the thrust bucket of the SSME mission could result in extreme structural loading on the orbiter vehicle with possible loss of mission if an accommodation strategy does not allow completion of the transient. To accomplish the accommodation, an off-nominal control may be designed which makes use of the remaining valves (OPOV, MOV, MFV, CCV, and OPFV) to provide closed loop control of MR and P_c while ignoring turbine discharge temperatures. Once the on-line diagnostic system has diagnosed the failure and estimated the position of the failed valve, the coordinator can compute the maximum possible P_c for the engine without forcing MR off nominal (6.011). The coordinator generates new commands for the engine and initiates control blending using the approach outlined above. Once control reconfiguration is complete, the off nominal control provides variable throttling and MR control throughout the remainder of the mission with a new limit on maximum thrust for that engine.

The off-nominal controller without the FPOV is synthesized using the same control

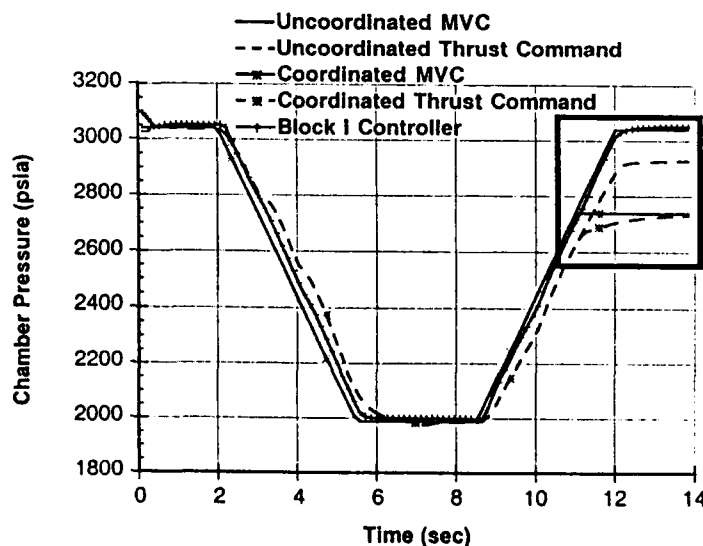


Figure 6 Chamber Pressure Response for Thrust Bucket with Valve Failure

structure, design methodology and sensor suite employed with the nominal controller. Control of MR without using the FPOV is a very difficult task since the MR response depends heavily on this valve. In fact, the Block I control uses FPOV exclusively for MR regulation. The design procedure¹⁰ resulted in a controller of the same order as the nominal control and uses four valves (OPOV, CCV, OPFV and MFV) to decouple the MR from the P_c response. Theoretically, decoupling using fewer valves is possible. However the objective was to demonstrate the capability of recovering from a failure in a primary control valve while preserving control of P_c and MR. The off nominal control performs satisfactorily over mainstage without gain scheduling as does the nominal control.

Figures 6 and 7 show the P_c and MR responses for the thrust bucket maneuver, respectively. Figure 6 includes five curves with two sets of two being identical until after approximately the eleven second mark and are highlighted with a rectangle. The coordinated and uncoordinated MVC and thrust command demonstrate the importance of the engine level coordination. The Block I controller response is included for reference purposes to motivate the need for accommodation. The failure of FPOV occurs at exactly three seconds into the transient when the valve locks up. The responses shown assume identification takes place instantly which is certainly unrealistic. The plots show the best you can do with the reconfigurable MVC. Any delay in identification will degrade the performance of the accommodation scheme. Very little perturbation is seen during accommodation of the valve by the MVC while the Block I control is smooth since OPOV is responsible for P_c control. Figure 7 shows the degradation in MR control when the valve sticks for both MVC and Block I. However, reconfiguration of the MVC by four seconds (blending) begins to return MR to the design point while the Block I response shows the coupling between P_c and MR.

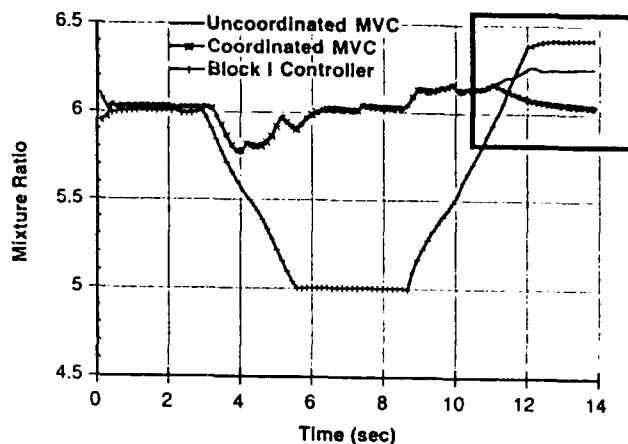


Figure 7 Mixture Ratio Response for Thrust Bucket with Valve Failure

If the coordinator does not lower the maximum P_c for the engine based on the position of FPOV then the responses shown for the "Uncoordinated MVC" result. Figures 6 and 7 show the tradeoff between P_c and MR when "too much" thrust is requested from the engine. Neither P_c or MR can meet demand, therefore the MVC balances the errors based upon the relative weights used in the design procedure. The imbalance is exemplified by the Block I control which meets requested thrust while MR in Figure 7 increases to 7% over nominal. If coordination takes place, then the responses labelled "Coordinated MVC" result. Figure 6 shows how a decrease in demanded thrust for the MVC can be achieved while keeping MR in Figure 7 at or about the nominal setting. A decrease in demanded thrust by a particular engine in a propulsion system can be compensated for by other "healthy" engines in the cluster without compromising the mission.

INTELLIGENT CONTROLS GRAPHICAL USER INTERFACE

The Graphical User Interface (GUI) was developed to allow the ICS to be monitored during operation. The GUI permits operators to observe the ICS in real-time operation as it accommodates faults in components, sensors, and actuators, using a collection of screens designed to provide a clear illustration-through plots, text, and animation-of the entire process. The GUI is a full-color, object-oriented system consisting of a set of screens arranged hierarchically. Each screen consists of three windows: a mouse-sensitive graphical display window containing a diagram of a component or system, a plotting window depicting time responses of key variables associated with that component or system, and an interactive type-out window displaying messages and allowing the user to enter commands. When the mouse pointer is over a selectable object in the mouse-sensitive graphical display window, a box appears around the object and its name is displayed at the bottom of the screen. Clicking on it brings

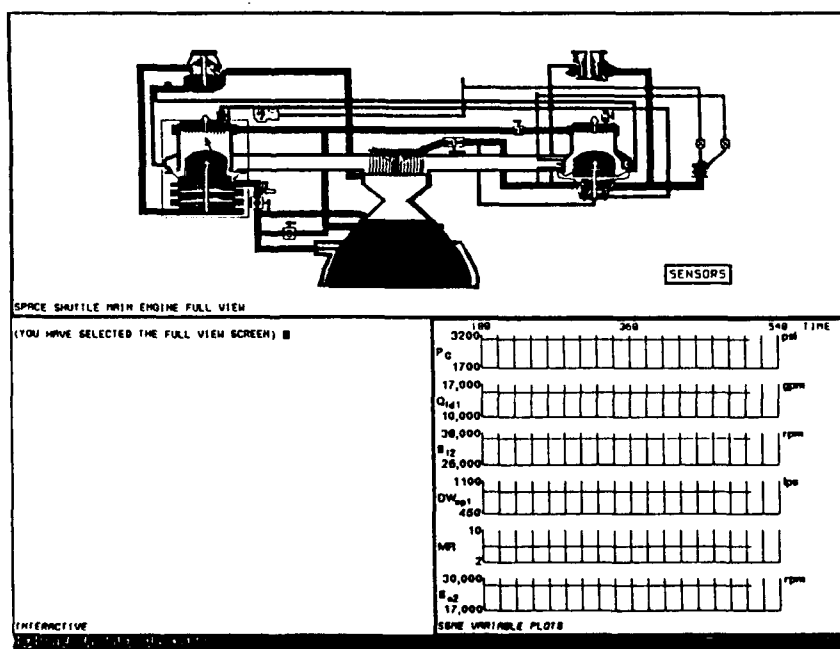


Figure 8 Main Screen for the Intelligent Control System Graphical User Interface

Each screen consists of three windows: a mouse-sensitive graphical display window containing a diagram of a component or system, a plotting window depicting time responses of key variables associated with that component or system, and an interactive type-out window displaying messages and allowing the user to enter commands. When the mouse pointer is over a selectable object in the mouse-sensitive graphical display window, a box appears around the object and its name is displayed at the bottom of the screen. Clicking on it brings

up the screen corresponding to the object. The hierarchy of screens may be viewed in this manner. Figure 8 shows an example screen. The top window contains a view of the space shuttle main engine composed of selectable objects, the window on the lower left displays messages, and that on the lower right displays plots. One of the components is selected as indicated by the box around it and its name is displayed in the lower left corner of the figure. The GUI plots time responses of important variables and indicates failures to the user through messages in the type-out window and by causing failed mouse-selectable components to flash. The user may bring up more detailed screens by clicking on the objects. Because of the modular, object-oriented nature of the GUI, the creation of additional screens is simple and quick. Thus appropriate screens can be added easily as more failure modes are incorporated into the testbed system.

SUMMARY

Demonstration of an Intelligent Control System for reusable rocket engines (SSME) is on-going at NASA LeRC. To facilitate this process, a preliminary subset of failure modes was selected from the set of all accommodatable failure modes. In particular, failure of a control sensor (P_c), a frozen Fuel Preburner Oxidizer Valve, a Low Pressure Fuel Turbo Pump shaft seal failure, a High Pressure Fuel Turbo Pump turbine tip seal failure, and a High Pressure Oxidizer Turbo Pump shaft seal failure were selected. Due to the requirement of accommodating engine failures or degradations, hot fire data cannot be used in closed loop evaluation and serves to validate health monitoring algorithms only. Consequently, a modelling effort is ongoing to study the effects of the failures on SSME performance and some results to date have been included. Modelling has focused on first order effects and little attention has been paid to the propagation of failures or the potential negative impact of off nominal operation of the engine and subsequent failures. These are important issues, however our focus is constrained given available resources to address this complex problem. The failure models are used to study the behavior of the engine as a failure occurs during closed loop operation with a nominal engine controller. If unacceptable behavior results, the operating point or the set of controlled variables or both is changed to accommodate the problem by the engine level coordinator. If none of these actions resolves the anomalous behavior, an alternate control design is performed off-line to meet the requirement of fault tolerance. A reconfiguration scheme has been presented which allows switching between predesigned controllers running in parallel based on the identified engine failure. An example using a stuck Fuel Preburner Oxidizer Valve was given to illustrate these ideas on a realtime simulation of the SSME. Results show that successful accommodation of primary control valves can be achieved using control reconfiguration in conjunction with a multivariable design methodology. Finally, the graphical user interface for the Intelligent Control System project was presented which aides the analysis of the system during accommodation of simulated engine failures.

REFERENCES

1. Cikanek, H. A., "Characteristics of Space Shuttle Main Engine Failures," AIAA-87-1939, 23rd Joint Propulsion Conference, San Diego, CA., 29 June - 2 July 1987.
2. Merrill, Walter C. and Lorenzo, Carl F. "A Reusable Rocket Engine Intelligent Control," AIAA-88-3114, 24 Joint Propulsion Conference, Boston, MA., July 11-13, 1988.
3. Merrill, W.C., Musgrave, J.L., and Guo, T.H., "Integrated Health Monitoring and Controls for Rocket Engines," 921031, 1992 SAE Aerospace Atlantic Conference, Dayton, OH., April 7-10, 1992.
4. Guo, T.H., Merrill, W.C., and Dwyer, A. "Real-Time Diagnostics for a Reusable Rocket Engine," 1992 Conference on Advanced ETO Propulsion Technology, NASA MSFC, May 19-21, 1992.
5. Nguyen, D.G. "Engine Balance and Dynamic Model," Rocketdyne Division, Rockwell International Corp., Report RL-00001, Version G and H.
6. Paxson, D.E., "A Model for the Space Shuttle Main Engine High Pressure Oxidizer Turbopump Shaft Seal System," Second Annual Conference on Health Monitoring for Space Propulsion Systems, Cincinnati, Ohio, Nov. 14-15, 1990.
7. Roelke, R.J. "Miscellaneous Losses" in Turbine Design and Application, ed. Arthur Glassman, NASA SP-29, Vol. II, 1972, pp. 125.
8. System Controls Technology Inc., "Failure Modes Definition for Reusable Rocket Engine Diagnostic System," NASA Contract No. NAS3-25813, June 1990.
9. Nemeth, Ed. "Reusable Rocket Engine Intelligent Control System Framework Design," NASA CR187043, April 6, 1991.
10. Musgrave, J.L. "Linear Quadratic Servo Control of a Reusable Rocket Engine," to appear in the Journal of Guidance, Control and Dynamics, Summer 1992.
11. Lorenzo, C.F. and Musgrave, J.L. "Overview of Rocket Engine Control," Ninth Symposium on Space Nuclear Power Systems, Albuquerque, New Mexico, Jan. 12-16, 1992.
12. Moerder, D.D., et. al. "Application of Precomputed Control Laws in a Reconfigurable Aircraft Flight Control System," Journal of Guidance, Navigation, and Control, Vol. 12, No.3, May-June 1989, pp. 325-333.

REPORT DOCUMENTATION PAGE			Form Approved OMB No. 0704-0188	
Public reporting burden for this collection of information is estimated to average 1 hour per response, including the time for reviewing instructions, searching existing data sources, gathering and maintaining the data needed, and completing and reviewing the collection of information. Send comments regarding this burden estimate or any other aspect of this collection of information, including suggestions for reducing this burden, to Washington Headquarters Services, Directorate for Information Operations and Reports, 1215 Jefferson Davis Highway, Suite 1204, Arlington, VA 22202-4302, and to the Office of Management and Budget, Paperwork Reduction Project (0704-0188), Washington, DC 20503				
1. AGENCY USE ONLY (Leave blank)	2. REPORT DATE June 1992	3. REPORT TYPE AND DATES COVERED Technical Memorandum		
4. TITLE AND SUBTITLE A Demonstration of an Intelligent Control System for a Reusable Rocket Engine		5. FUNDING NUMBERS WU-582-01-11		
6. AUTHOR(S) Jeffrey L. Musgrave, Daniel E. Paxson, Jonathan S. Litt, and Walter C. Merrill				
7. PERFORMING ORGANIZATION NAME(S) AND ADDRESS(ES) NASA Lewis Research Center Cleveland, Ohio 44135-3191 and Propulsion Directorate U.S. Army Aviation Systems Command Cleveland, Ohio 44135-3191		8. PERFORMING ORGANIZATION REPORT NUMBER E-7224		
9. SPONSORING/MONITORING AGENCY NAMES(S) AND ADDRESS(ES) National Aeronautics and Space Administration Washington, D.C. 20546-0001 and U.S. Army Aviation Systems Command St. Louis, Mo. 63120-1798		10. SPONSORING/MONITORING AGENCY REPORT NUMBER NASA TM-105794		
11. SUPPLEMENTARY NOTES Preprint from the "Advanced Earth-to-Orbit Propulsion Technology Conference," a conference held at NASA George C. Marshall Space Flight Center, Huntsville, Alabama, May 19-21, 1992. Jeffrey L. Musgrave and Daniel E. Paxson, NASA Lewis Research Center, Cleveland, Ohio; Jonathan S. Litt, Propulsion Directorate, U.S. Army Aviation Systems Command, Cleveland, Ohio; Walter C. Merrill, NASA Lewis Research Center. Responsible person, Jeffrey L. Musgrave, (216) 433-6472.				
12a. DISTRIBUTION/AVAILABILITY STATEMENT Unclassified - Unlimited Subject Category 20			12b. DISTRIBUTION CODE	
13. ABSTRACT (Maximum 200 words) An Intelligent Control System for reusable rocket engines is under development at NASA Lewis Research Center. The primary objective is to extend the useful life of a reusable rocket propulsion system while minimizing between flight maintenance and maximizing engine life and performance through improved control and monitoring algorithms and additional sensing and actuation. This paper describes current progress towards proof-of-concept of an Intelligent Control System for the Space Shuttle Main Engine. A subset of identifiable and accommodatable engine failure modes is selected for preliminary demonstration. Failure models are developed retaining only first order effects and included in a simplified nonlinear simulation of the rocket engine for analysis under closed loop control. The engine level coordinator acts as an interface between the diagnostic and control systems, and translates thrust and mixture ratio commands dictated by mission requirements, and engine status (health) into engine operational strategies carried out by a multivariable control. Control reconfiguration achieves fault tolerance if the nominal (healthy engine) control cannot. Each of the aforementioned functionalities is discussed in the context of an example to illustrate the operation of the system in the context of a representative failure. A graphical user interface allows the researcher to monitor the Intelligent Control System and engine performance under various failure modes selected for demonstration.				
14. SUBJECT TERMS Intelligent control; Failure mode modelling; Reconfigurable controls			15. NUMBER OF PAGES 10	
			16. PRICE CODE A02	
17. SECURITY CLASSIFICATION OF REPORT Unclassified	18. SECURITY CLASSIFICATION OF THIS PAGE Unclassified	19. SECURITY CLASSIFICATION OF ABSTRACT Unclassified	20. LIMITATION OF ABSTRACT	